

A Test of the Collisional Dark Matter Hypothesis from Cluster Lensing

Jordi Miralda-Escudé¹

Ohio State University, Dept. of Astronomy, McPherson Labs., 140 W. 18th Ave., Columbus, OH
43210

¹ Alfred P. Sloan Fellow

ABSTRACT

Spergel & Steinhardt proposed the possibility that the dark matter particles are self-interacting, as a solution to two discrepancies between the predictions of cold dark matter models and the observations: first, the observed dark matter distribution in some dwarf galaxies has large, constant-density cores, as opposed to the predicted central cusps; and second, small satellites of normal galaxies are much less abundant than predicted. The dark matter self-interaction would produce isothermal cores in halos, and would also expel the dark matter particles from dwarfs orbiting within large halos. However, another inevitable consequence of the model is that halos should become spherical once most particles have interacted. Here, I rule out this model by the fact that the innermost regions of dark matter halos in massive clusters of galaxies are elliptical, as shown by gravitational lensing and other observations. The absence of collisions in the lensing cores of massive clusters implies that any dark matter self-interaction is too weak to have affected the observed density profiles in the dark-matter dominated dwarf galaxies, or to have eased the destruction of dwarf satellites in galactic halos. If s_x is the cross section and m_x the mass of the dark matter particle, then $s_x/m_x < 10^{-25.5} \text{ cm}^2/\text{GeV}$.

Subject headings: galaxies: formation - large-scale structure

1. Introduction

The Cold Dark Matter (hereafter, CDM) model of structure formation in the universe has been tremendously successful in accounting for a huge variety of available observations, (the Cosmic Background fluctuations, the abundances of clusters of galaxies, the peculiar velocity fields, the Ly α forest, ...), provided that the mean density of matter is only a fraction $\Omega_m \simeq 0.3$ of the critical density, and the existence of vacuum energy with a negative pressure equation of state is allowed to make the universe spatially flat (e.g., Perlmutter, Turner, & White 1999; Bahcall et al. 1999; Strauss & Willick 1995; Eke, Cole, & Frenk 1996; Croft et al. 1999).

A possible problem with this model has emerged when comparing the density profiles of dark matter halos predicted in numerical simulations, with observations of the rotation curves in dwarf

galaxies (Moore 1994; Flores & Primack 1994; Navarro, Frenk, & White 1996; Moore et al. 1998; Kravtsov et al. 1998; Moore et al. 1999b). Whereas the observations show linearly rising rotation curves out to core radii greater than 1 kpc in certain dwarf galaxies where the density is dominated by dark matter everywhere (indicating that the dark matter has a constant density core), the simulations predict that the collapse of collisionless particles of cold dark matter produces halo density profiles that are steeper in the central parts, never decreasing their logarithmic slope below 1.5 in the highest resolution simulations. In addition, a problem also appears when attempting to fit the rotation curves of more massive galaxies when the dark matter halo is constrained to have the shape predicted in simulations (Navarro & Steinmetz 2000): when the stellar mass is added to that of the dark matter halo, the resulting overall mass distribution is also too centrally concentrated to fit the observed rotation curves. A second problem is that the number of dwarf galaxies observed in the Local Group is much smaller than the total number predicted from numerical simulations (Klypin et al. 1999; Moore et al. 1999b).

A solution to this discrepancy was recently proposed by Spergel & Steinhardt (1999): if the dark matter is self-interacting, with a sufficiently large cross section for elastic scattering so that most particles in the inner core of a dwarf galaxy would have interacted among themselves over a Hubble time, then an isothermal core will be produced. Notice that any interaction of the dark matter particle with the baryonic matter must be much rarer than this proposed self-interaction in order to satisfy the limits of the dark matter detection experiments; also, inelastic scattering of the dark matter particles should be rare to prevent the dark matter from dissipating energy and becoming more centrally concentrated.

One of the clear predictions of the hypothesis that the dark matter is collisional, as mentioned by Spergel & Steinhardt (1999), is that when most of the particles of a halo within some radius have interacted, then the halo should be almost spherical, or else be supported by rotation, because the velocity dispersion tensor should become isotropic. This paper examines the consequence of this prediction for the inner parts of rich clusters of galaxies, where highly magnified images of background galaxies are occasionally observed. We will find that this places severe restrictions on the collisional dark matter hypothesis, ruling out its possible role in explaining the observed cores in the density profiles of dwarf galaxies.

2. The Collisional Radius in Dwarf Galaxies and in Galaxy Clusters

Let us assume that at some initial time, a dark matter halo has the density profile obtained in numerical simulations, which will thereafter be changed by the effects of the collisions of the dark matter particles. This initial density profile has a characteristic radius r_h , such that the logarithmic slope is $|d \log \rho / d \log r| < 2$ at $r < r_h$, and $|d \log \rho / d \log r| > 2$ at $r > r_h$ (Navarro, Frenk, & White 1996; Moore et al. 1999b). The particles closest to the center will be the first ones to collide, owing to the higher density. We define the collisional radius, r_c , as the radius within which more than half the particles have interacted. The effects of the collisions will be to change

the velocity distribution of the particles inside the collisional radius to a Maxwellian distribution, with constant velocity dispersion. This implies that the density profile within the collisional radius will be altered to that of an isothermal sphere with finite core.

In the initial density profile, the velocity dispersion should clearly decrease toward the center at $r < r_h$: as long as the density profile has a central power-law cusp, and the orbits are not all highly radial near the center, then $\sigma^2(r) \propto \rho(r)r^2$. The collisions will therefore transport heat to the colder central particles from the hotter exterior, destroying the cusp and slowly increasing the core of the isothermal sphere as the collisional radius increases. However, the particles at $r > r_h$ should have a decreasing velocity dispersion with radius in their initial configuration, so when $r_c > r_h$ heat starts to be transported outward and the isothermal core shrinks as more particles are slung to the outer parts of the halo (or to unbound orbits), leading eventually to core collapse. As discussed by Spergel & Steinhardt (1999), the cross section should be low enough so that the core collapse of the dark matter has not taken place in any halos up to the present time.

How should the collisional radius vary with the velocity dispersion of a dark matter halo? Clearly, the rate of interaction of a particle is proportional to the dark matter density, ρ , times the velocity dispersion σ . Hence, $\rho \sigma t = \text{constant}$, where t is the age of the halo. Assuming that the core of the halo is not larger than the collisional radius, $\rho(r_c) \propto \sigma^2/r_c^2$, and therefore,

$$r_c \propto \sigma^{3/2} t^{1/2} . \quad (1)$$

This implies that *if the core radii in dwarf galaxies are caused by dark matter collisions, then all the galactic and cluster dark matter halos should have much larger core radii as their velocity dispersion increases.*

Typically, the constant density cores of dwarf galaxy halos measured from the kinematics of the HI gas extend out to a few kpc, and a typical velocity dispersion is 50 km s^{-1} . As a few examples, the rotation curves of the dwarfs DDO 154, DDO 170, and DDO 236 yield fits for their dark matter halos with velocity dispersion $\sigma = (28, 52, 45) \text{ km s}^{-1}$, and core radii (3, 2.5, 6) kpc (Carignan & Beaulieu 1989; Lake, Schommer, & van Gorkom 1990; Jobin & Carignan 1990), with assumed distances of (4, 15, 1.7) Mpc, respectively.

If we wish to explain the sizes of these dark matter cores in dwarf galaxies as the result of collisional dark matter, then we must conclude that much larger cores must exist in rich clusters of galaxies due to the same process. Using the conservative values of $r_c = 2 \text{ kpc}$ and $\sigma = 50 \text{ km s}^{-1}$ for a typical dwarf galaxy, and assuming (also conservatively) that a typical rich cluster will be only about a third as old as a dwarf galaxy (since rich clusters should have collapsed at a later time than dwarf galaxies), we infer that the collisional radius of a typical rich cluster with velocity dispersion $\sigma = 1000 \text{ km s}^{-1}$ should be at least $r_c > 100 \text{ kpc}$.

Within the collisional radius, the halo potential should be very nearly spherical because the collisions should make the velocity dispersion tensor of the dark matter particles isotropic (unless the core is rapidly rotating, which is highly unlikely as will be discussed in §4). The next section

discusses the evidence from gravitational lensing showing that clusters are elliptical in general, and they do not become spherical in their central parts.

3. The core of the cluster MS2137-23 is elliptical

Highly magnified images of background galaxies (or “arcs”) produced by gravitational lensing have been observed in many clusters of galaxies. In general, models that reproduce the positions and shapes of these images assume the presence of elliptical clumps of dark matter centered on the most luminous galaxies in the cluster, with the ellipticity being oriented along the same axis as the optical light. Examples of clusters that have been modeled in this way include A370 (Kneib et al. 1993), A2218 (Kneib et al. 1995), and MS2137-23 (Mellier, Fort, & Kneib 1993). The lensing models in all these cases would not be successful in reproducing the observations if the dark matter around the luminous galaxies was assumed to be spherically distributed.

Here, we shall focus on the cluster MS2137-23. This cluster has several characteristics that make it particularly useful for our purpose: The central region of the cluster appears to be well relaxed, dominated by the central galaxy. Five gravitationally lensed images arising from two sources are observed, which can be accurately reproduced by a model of a simple elliptical potential with the same major axis as the central galaxy. One source produces a long, tangential arc and two other arclets, and the second source gives rise to a radially elongated image near the center and another arclet (where “arclet” refers to images that are not magnified by very large factors, but still show a characteristic stretching effect due to lensing). Finally, the presence of the radial image allows to obtain special constraints on the shape of the dark matter halo.

The simple fact that an elliptical potential, with constant ellipticity as a function of radius, is required to fit the positions and shapes of these five lensed images (Mellier et al. 1993; Miralda-Escudé 1995; Hammer et al. 1997) can already be considered as persuasive evidence that the potential cannot be spherical within ~ 100 kpc (the five gravitationally lensed images are within $100h^{-1}$ kpc of the cluster center). However, in order to illustrate the evidence that the inner part of the dark matter in this cluster cannot be spherical in a model-independent manner, using a simple analytical method, we will focus here on the radial image and its counterimage. These two images of the same source are labeled as A1 and A5 in Mellier et al. (1993), and in Figure 1 of Miralda-Escudé (1995), and as AR and A5 in the HST image presented in Hammer et al. (1997).

A schematic representation of the lensing of the source on the radial caustic is shown in Figure 1, which defines the notation that will be used here. The point labeled C is the center of the cluster, and S is the position of the source that gives rise to the radial image at R and the counterimage at I (the entire lensing configuration in this system, with the critical lines and caustics of a simple elliptical potential, is shown in Fig. 1 of Miralda-Escudé (1995)). We use polar coordinates on the image plane: θ , the angular distance from the center C , and ϕ , the azimuthal angle. The light ray observed at R is deflected by an angle $\alpha_{\theta R}$ in the radial direction, and $\alpha_{\phi R}$ in

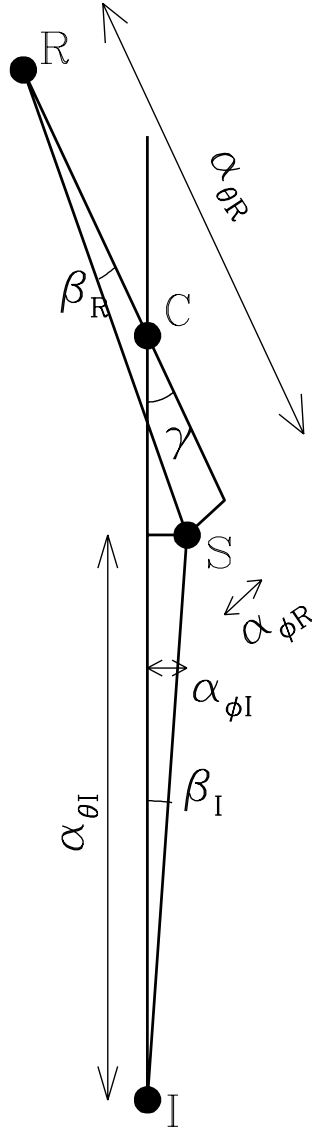


Fig. 1.— Schematic representation of the lensing configuration in the cluster MS2137-23 discussed in §3. The lens center is at C , the source is located at S , and its two images are observed at R (which is the image on the radial critical line) and I . The angle of misalignment γ between the two images relative to the center would be zero for a spherical potential. The radial and azimuthal components of the deflection angles (α_θ and α_ϕ) are indicated.

the azimuthal direction, and the same for the light ray observed at I .

The specific observed quantity that we will relate to the ellipticity of the potential is the angle γ of misalignment between the images R and I , relative to the center of the lens. In a spherical potential, the images R and I should lie on a straight line passing through C . The observed angle is $\gamma = 19^\circ$, indicating that the potential is elliptical. In principle, this misalignment could also be caused by substructure in the cluster, but this is unlikely in view of the relaxed appearance of the cluster.

We now relate the angle γ to the ellipticity and the density profile of the potential. If the ellipticity ϵ is small, the projected potential is adequately approximated with a quadrupole term (e.g., Miralda-Escudé 1995),

$$\psi(\theta, \phi) = \psi_0(\theta) - \frac{\epsilon}{2} \psi_1(\theta) \cos(2\phi) , \quad (2)$$

where

$$\psi_0(\theta) = \int_0^\theta d\theta' \alpha_0(\theta') , \quad (3)$$

$$\alpha_0(\theta) = \frac{2}{\theta} \int_0^{\theta'} d\theta' \theta' \kappa_0(\theta') \equiv \theta \bar{\kappa}_0(\theta') , \quad (4)$$

$$\psi_1(\theta) = \frac{2}{\theta^2} \int_0^\theta d\theta' \theta'^3 \kappa_0(\theta') , \quad (5)$$

and where the surface density of the lens is

$$\kappa(\theta, \phi) = \kappa_0(\theta) - \frac{\epsilon}{2} \theta \frac{d\kappa_0}{d\theta} \cos(2\phi) . \quad (6)$$

Here, $\kappa_0(\theta)$ is the azimuthally averaged surface density profile, and $\bar{\kappa}_0(\theta)$ is the averaged surface density within θ . The deflection angle is given by the gradient of the potential,

$$\alpha_\theta = \theta \bar{\kappa}_0(\theta) + \theta \left[\kappa_0(\theta) + \frac{\psi_1(\theta)}{\theta^2} \right] \epsilon \cos(2\phi) , \quad (7)$$

$$\alpha_\phi = \frac{\psi_1(\theta)}{\theta} \epsilon \sin(2\phi) . \quad (8)$$

In the limit of a small ellipticity of the potential, the angle of misalignment γ is given by (using the notation in Fig. 1),

$$\gamma = \beta_I \frac{\alpha_{\theta I}}{\theta_I - \alpha_{\theta I}} + \beta_R \frac{\alpha_{\theta R}}{\alpha_{\theta R} - \theta_R} = \frac{\alpha_{\phi I}}{\theta_I - \alpha_{\theta I}} + \frac{\alpha_{\phi R}}{\alpha_{\theta R} - \theta_R} . \quad (9)$$

Using the condition that the rays at images R and I are deflected to the same position S , which is simply $\theta_i - \alpha_{\theta I} = \alpha_{\theta R} - \theta_R$ (the ellipticity introduces only second order corrections here), we obtain

$$\gamma = \left[\frac{\psi_1(\theta_R)}{\theta_R} + \frac{\psi_1(\theta_I)}{\theta_I} \right] \frac{\epsilon \sin(2\phi_I)}{\theta_I - \alpha_{\theta I}} . \quad (10)$$

We now want to find a lower limit to the ellipticity necessary to generate the observed angle γ . For this purpose, it will be convenient to replace the function $\psi_1(\theta)/\theta$ by an upper limit. Using equation (5), we find that if the κ_0 is constant within θ , then $\psi_1(\theta)/\theta = \theta \bar{\kappa}_0(\theta)/2$, while in any profile where κ_0 decreases with radius, we have $\psi_1(\theta)/\theta < \theta \bar{\kappa}_0(\theta)/2$, because the integral of equation (5) weights more heavily the surface density near θ than at smaller angular radius. Therefore,

$$\gamma < \frac{[\theta_R \bar{\kappa}_0(\theta_R) + \theta_I \bar{\kappa}_0(\theta_I)] \epsilon \sin(2\phi_I)}{2 \theta_I [1 - \bar{\kappa}(\theta_I)]} = \frac{(1 + \theta_R/\theta_I) \epsilon \sin(2\phi_I)}{2 [1 - \bar{\kappa}(\theta_I)]}. \quad (11)$$

We can now substitute the observed values $\theta_I = 22''.5$ (Fort et al. 1992), and $\theta_R = 5''.2$ (Hammer et al. 1997):

$$\gamma < 0.62 \frac{\epsilon \cos(2\phi_I)}{1 - \bar{\kappa}_0(\theta_I)}. \quad (12)$$

To obtain a lower limit to ϵ , we need to assume an upper limit for $1 - \bar{\kappa}(\theta_I)$. Because the two images R and I result from radial (rather than tangential) magnification, there is no reason why $\bar{\kappa}$ needs to be particularly close to unity at either image. Given the relation $[\bar{\kappa}_0(\theta_R) - 1]/[1 - \bar{\kappa}_0(\theta_I)] = \theta_I/\theta_R = 4.3$, the quantity $1 - \bar{\kappa}(\theta_I)$ could be very small only if the surface density profile was very flat between the angular radii θ_R and θ_I . This is very unlikely because the velocity dispersion implied for the cluster for an Einstein radius close to $\theta_I = 22''.5$ is already larger than 1000 km s^{-1} (see Miralda-Escudé 1995, Figs. 8 and 9), and it would increase to a much higher value at large radius if the slope of the density profile was much shallower than isothermal at $\theta \sim \theta_I$.

As a reasonable limit on how flat the $\bar{\kappa}$ profile could be from θ_R to θ_I , we will assume here $\bar{\kappa}(\theta_R)/\bar{\kappa}(\theta_I) > 2$ (remember that $\theta_I/\theta_R = 4.3$). This corresponds to $1 - \bar{\kappa}_0(\theta_I) > 0.16$, implying that the image I is not tangentially magnified by more than a factor 6, which is reasonable given the length of the image I (called A5 in Hammer et al. 1997), $\sim 3''$, and its axis ratio of ~ 3 .

With this condition, and using also $\cos(2\phi_I) \simeq 0.7$ (e.g., Mellier et al. 1993; we assume the major axis of the potential is aligned with that of the central galaxy), and $\gamma = 0.33$, the lower limit on the ellipticity from equation (12) is

$$\epsilon > 0.77(1 - \bar{\kappa}(\theta_I)) \gtrsim 0.1. \quad (13)$$

4. Discussion

The multiple images of background galaxies produced by gravitational lensing in clusters of galaxies generally require elliptical models of the mass distribution in order to reproduce their positions and magnifications successfully. The last section discussed the specific example of MS2137-23, where the misalignment in the position of two images relative to the cluster center can be used to constrain the ellipticity in a model-independent way: the ellipticity of the dark matter halo around the central galaxy must be greater than 0.1 within the image I , which is at $22''.5$ from

the cluster center, corresponding to a distance of $65h^{-1}$ kpc. The fact that the dark matter halos of galaxy clusters are elliptical within this small radius implies that the dark matter particles have not collided over the age of the cluster. As shown in §2, this also implies that the observed cores of the dark matter halos in dwarf galaxies are too big to have been caused by collisions of the dark matter, as proposed by Spergel & Steinhardt (1999).

Further evidence supporting that cluster dark matter halos have roughly a constant ellipticity at all radii comes from the similarity with the ellipticity of the isophotes of the central cluster galaxies in both the magnitude of the ellipticity and the orientation of the major axis (Mellier, Fort, & Kneib 1993; Hammer et al. 1997). If the underlying dark matter distribution became spherical due to the collisions, the ellipticity of the stellar distribution would be reduced (although not eliminated, owing to the anisotropy in the velocity dispersion tensor). According to Hammer et al. (1997), the central galaxy in MS2137-23 has ellipticity $\epsilon = 0.16 \pm 0.02$ beyond the radius of the radial arc, and the best fit ellipticity for the lens model is $\epsilon = 0.18$ (see also Kneib et al. 1995 for similar conclusions obtained in the cluster A2218).

The ellipticity of the cluster halo can be used to place an upper limit on the interaction rate of the dark matter, in terms of the cross section s_x and mass m_x of the dark matter particle. We assume here that the collisional radius must be smaller than the distance from the center of the long tangential arc and two other arclets (these images are A01-A02, A2 and A4 in Hammer et al. 1997, and they also require an ellipticity similar to that of the central galaxy in the lensing models), which is about $15''$, or a radius $r \sim 70$ kpc (we use $H_0 = 65 \text{ km s}^{-1} \text{ Mpc}^{-1}$). The dark matter density at this radius is $\rho \simeq \Sigma_{crit}/2r$, where the critical surface density is $\Sigma_{crit} \simeq 1 \text{ g cm}^{-2}$ for a source at $z_s = 1$. Assuming also a cluster velocity dispersion $\sigma = 1000 \text{ km s}^{-1}$ (roughly the minimum value required given the Einstein radius of the cluster), and a cluster age $t_c = 5 \times 10^9$ years, we obtain the upper limit

$$\frac{s_x}{m_x} < \frac{1}{\rho 2^{1/2} \sigma t_c} \simeq 10^{-25.5} \frac{\text{cm}^2}{m_p} \simeq 0.02 \frac{\text{cm}^2}{\text{g}} . \quad (14)$$

For the dwarf galaxies DDO 154, DDO 170, and DDO 236 mentioned in §2, with velocity dispersion $\sigma = (28, 52, 45) \text{ km s}^{-1}$, and core radii (3, 2.5, 6) kpc, the time it would take for the collisional radius to reach the value of their core radii if s_x/m_x were equal to the above upper limit is $t = (40, 5, 40) \times 10^{10}$ years, respectively [where we have used the relation $t \propto \sigma^3/r_c^2$, from eq. (1)].

This limit we have obtained on the self-interaction of the dark matter also rules it out as an explanation for the low abundance of dwarf galaxies in the Local Group, compared to the predictions of halo satellites abundances from numerical simulations (Klypin et al. 1999; Moore et al. 1999a). In order to strike out the dark matter particles, the satellite halos must be moving in an orbit inside the collisional radius. For example, in the Milky Way halo (with $\sigma \simeq 150 \text{ km s}^{-1}$), the collisional radius cannot be greater than about 6 kpc, if $r_c < 100$ kpc in a cluster with $\sigma = 1000 \text{ km s}^{-1}$ (where we use the scaling $r_c \propto \sigma^{3/2}$).

Does there remain any possibility of saving the collisional dark matter hypothesis as an explanation of the constant density cores observed in some dwarf galaxies? A possible argument that could be made is that the presence of substructure in the mass distribution of MS2137-23, or of other massive structures projected on the line of sight of the cluster, might introduce an external shear that would modify the positions of the images. However, external shear could not mimic the positions predicted by an intrinsic ellipticity for all the observed images, and would also not explain why the stellar distribution is elliptical with the same orientation that is predicted for the potential. Another possibility would be that the ellipticity of the dark matter halo in MS2137-23 is induced by rotation, with an isotropic velocity dispersion for the dark matter. However, halos formed by collisionless collapse are known to rotate very slowly (Barnes & Efstathiou 1987; Warren et al. 1992), and the collisions would further slow down the rotation of the central parts of the halo by enforcing solid body rotation. Therefore, it seems that the discrepancy between the constant density cores observed in dwarf galaxies and the cuspy density profiles predicted for dark matter halos in simulations of cold dark matter require a different explanation.

I am grateful to Andy Gould, Paul Steinhardt and David Weinberg for discussions and for their encouragement.

REFERENCES

- Bahcall, N., Ostriker, J. P., Perlmutter, S., & Steinhardt, P. J. 1999, *Science*, 284, 1481
- Barnes, J., & Efstathiou, G. 1987, *ApJ*, 319, 575
- Carignan, C., & Beaulieu, S. 1989, *ApJ*, 347, 760
- Croft, R. A. C., Weinberg, D. H., Pettini, M., Hernquist, L., & Katz, N. 1999, *ApJ*, 520, 1
- Eke, V. R., Cole, S., & Frenk, C. S. 1996, *MNRAS*, 282, 263
- Flores, R. A., & Primack, J. A. 1994, *ApJ*, 427, L1
- Fort, B., Le Fèvre, O., Hammer, F., & Cailloux, M. 1992, *ApJ*, 399, L125
- Hammer, F., Gioia, I. M., Shaya, E. J., Teyssandier, P., Le Fèvre, O., & Luppino, G. A. 1997, *ApJ*, 491, 477
- Jobin, M., & Carignan, C. 1990, *AJ*, 100, 648
- Klypin, A. A., Kravtsov, A. V., Valenzuela, O., & Prada, F. 1999, *ApJ*, 522, 82
- Kneib, J. P., Mellier, Y., Fort, B., & Mathez, G. 1993, *A&A*, 273, 367
- Kneib, J. P., Mellier, Y., Pelló, R., Miralda-Escudé, J., Le Borgne, J.-F., Böhringer, H., & Picat, J.-P. 1995, *A&A*, 303, 27
- Kravtsov, A. V., Klypin, A. A., Bullock, J. S., & Primack, J. R. 1998, *ApJ*, 502, 48
- Lake, G., Schommer, R. A., & van gorkom, J. A. 1990, *AJ*, 99, 547
- Mellier, Y., Fort, B., & Kneib, J. P. 1993, *ApJ*, 407, 33
- Miralda-Escudé, J. 1995, *ApJ*, 438, 514
- Moore, B. 1994, *Nat*, 370, 629
- Moore, B., Governato, F., Quinn, T., Stadel, J., & Lake, G. 1998, *ApJ*, 499, L5
- Moore, B., Ghigna, S., Governato, F., Lake, G., Quinn, T., Stadel, J., & Tozzi, P. 1999, *ApJ*, 524, L19 (astro-ph/9907411)
- Moore, B., Quinn, T., Governato, F., Stadel, J., & Lake, G. 1999, submitted to *MNRAS* (astro-ph/9903164)
- Navarro, J. F., Frenk, C. S., & White, S. D. M. 1996, *ApJ*, 462, 563
- Navarro, J. F., & Steinmetz, M. 2000, *ApJ*, in press (astro-ph/9908114)

- Perlmutter, S., Turner, M. S., & White, M. 1999, *Phys. Rev. Lett.*, 83, 670
- Spergel, D. N., & Steinhardt, P. J. 1999, *Phys. Rev. ???* (astro-ph/9909386)
- Strauss, M. A., & Willick, J. A. 1995, *Phys. Rep.*, 261, 271
- Warren, M. S., Quinn, P. J., Salmon, J. K., & Zurek, W. H. 1992, *ApJ* 399, 405